EUROPEAN ORGANIZATION FOR NUCLEAR RESEARCH

L3 Note 2577
July 6, 2000

Search for Single Top Production at LEP 2

The L3 Collaboration

Abstract

We report on the search for single top production in e^+e^- collisions, using the data corresponding to an integrated luminosity of 410 pb^{-1} collected by L3 in 1998 and 1999 at a mean center of mass energy of 193.3 GeV. We present two independent analysis in the purely hadronic and semileptonic top decay channels. Combining the results of both analysis, We quote a preliminary limit of $\sigma(e^+e^- \rightarrow t\bar{c}(\bar{u}) + c.c.) < 136$ fb at 95% confidence level.

Submitted to the *XXXth International Conference on High Energy Physics*
July 27 - August 2, 2000, Osaka, Japan

1 introduction

At LEP 2, the top quark can be produced only via the flavor changing neutral current (FCNC) processes $e^+e^- \rightarrow t\bar{c}(\bar{u})$. Within the standard model (SM) framework, such processes arise only through loops and are therefore highly suppressed [1, 2]. Thus, the FCNC single top production at LEP 2 is an ideal place to search for new physics which could lead to a significant increase of FCNC top interactions. Substantial enhancements, by some orders of magnitude, of FCNC top branching ratios, can be obtained in two or multiple higgs doublet models [1, 3] ($BR \simeq 10^{-9} \div 10^{-5}$), in super-symmetric models [4, 5] ($BR \simeq 10^{-8} \div 10^{-6}$), in quark singlets models [6] or in more exotic models as compositeness [7] ($BR \simeq 10^{-2}$).

Phenomenological limits on FCNC decays of the top quark have been set by the CDF collaboration [8]:

$$BR(t \rightarrow \gamma c/\gamma u) < 3.2\,\% \quad (95\%\ C.L.) \tag{1}$$

$$BR(t \rightarrow Zc/Zu) < 33\,\% \quad (95\%\ C.L.) \tag{2}$$

In this paper we refer to the model independent analyses of reference [9] that describe both processes in terms of anomalous couplings $tV_0\bar{c}$, $tV_0\bar{u}$, with $V_0 = \gamma, Z$. However, different kind of effective vertices such as the $tcee$ four-Fermi interactions could contribute in a significant way to enhance the $t\bar{c}(\bar{u})$ production at e^+e^-colliders and can be taken into account as well [10].

The vertices of the FCNC transition $\gamma/Z \rightarrow t\bar{c}(\bar{c})$ can be written as [1)]:

$$\Gamma^{\gamma}_{\mu} = k_{\gamma}\frac{ee_q}{\Lambda}\sigma_{\mu\nu}q^{\nu} \tag{3}$$

$$\Gamma^{Z}_{\mu} = k_{Z}\frac{e}{\sin(2\theta_W)}\gamma_{\mu} \tag{4}$$

where Λ is the new physics cutoff set to the top mass. k_γ and k_Z define the strength of the anomalous coupling, which are constrained by the CDF limits (1,2) to $k^2_\gamma < 0.176$ and $k^2_Z < 0.533$.

Using the expression of the anomalous vertices, it is straightforward to get the Born level cross section for the process $e^+e^- \rightarrow t\bar{c} + \bar{t}c$ (or $t\bar{u} + \bar{t}u$) [2)]:

$$\begin{aligned}\sigma(\mathrm{e^+e^-} \rightarrow t\bar{c}) \;=\; & \frac{\pi\alpha^2}{s}\left(1-\frac{m_t^2}{s}\right)^2\left[k_\gamma^2 e_q^2\frac{s}{m_t^2}\left(1-2\frac{m_t^2}{s}\right)+\right.\\ & + \left.\frac{k_Z^2(1+a_W^2)(2+m_t^2/s)}{4\sin^4(2\theta_W)(1-m_Z^2/s)^2} + 3k_z k_\gamma\frac{a_W e_q}{\sin^2(2\theta_W)(1-m_Z^2/s)}\right]\end{aligned} \tag{5}$$

2 Data and Montecarlo Samples

For this analysis, we have used the 410 pb^{-1} collected by L3 [11–19] at $\sqrt{s}$ =189 - 202 GeV, in years 1998 and 1999 (Figure 1). The signal sample is simulated using a modified version of JETSET [20]. We produce different samples of signal events for systematic studies, varying the top mass in the range 170÷180 GeV and adopting two extreme values for the forward–backward asymmetry ($A_{FB} = 0$ and $A_{FB} = 0.9$). For the background samples the following Montecarlo generators are used: PYTHIA [21, 22] for $e^+e^- \rightarrow q\bar{q}(\gamma)$ and $e^+e^- \rightarrow$ ZZ, KORALW [23, 24]

1) $e_q = 2/3$ is the charge fraction of t quark, θ_W is the Weinberg angle and $\sigma^{\mu\nu} = \frac{1}{2}(\gamma^\mu\gamma^\nu - \gamma^\nu\gamma^\mu)$

2) Where $a_W = 1 - 4sin^2\theta_W$. The calculations are made in the massless approximation for the $c(u)$ quark.

for $e^+e^- \rightarrow \mathrm{W}^+\mathrm{W}^-$, KORALZ [25] for $e^+e^- \rightarrow \tau^+\tau^-$. The L3 detector response is simulated using the GEANT program [26] which takes into account the energy loss, multiple scattering and showering in the detector. The GHEISHA program [27] is used to simulate hadronic interactions in the detector.

3 Analysis Procedures

Due to its large mass, at $\sqrt{s} \geq 189$ GeV the top quark is produced almost at rest in the reaction $e^+e^- \rightarrow t\bar{c}$. In addition, it decays quickly via $t \rightarrow Wb$, without forming top-flavoured hadrons. Depending on the successive decay of the W boson, the expected final state signatures are four-jets ($t\bar{c} \rightarrow Wb\bar{c} \rightarrow q\bar{q}'b\bar{c}$) or two jets, one lepton and missing energy ($t\bar{c} \rightarrow Wb\bar{c} \rightarrow l\nu b\bar{c}$), here referred as *hadronic* and *leptonic* channels. In both cases the energy of the $c-$ and $b-$jets are almost fixed at values:

$$E_c \simeq \frac{\sqrt{s}}{2}\left(1 - \frac{m_t^2}{s}\right) \tag{6}$$

$$E_b \simeq \frac{m_t}{2} - \frac{m_W^2}{2m_t} \tag{7}$$

In addition, both channels are characterised by the presence of a $b-$quark jet. A $b-$jet tagging algorithm [28] is used, which is mainly based on lifetime information.

Common search procedures are applied to both the leptonic and hadronic channels. First, a preselection is applied which significantly reduces background while keeping high signal efficiency. This is especially effective against background from low multiplicity events and from the two-photon interaction. Second, a final set of selections cuts is chosen to distinguish signal from background. Once the final selection has been applied, a discriminating variable is constructed using a neural-network technique or a likelihood method.

3.1 Leptonic Channel

The signature for this channel is one energetic lepton, large missing transverse momentum from the neutrino, two jets with large difference in energy, out of which one contains b quark. The main background is given by $e^+e^- \rightarrow W^+W^-$ and $e^+e^- \rightarrow q\bar{q}$.

High multiplicity hadronic events are selected with at least 3 tracks, more than 15 calorimetric clusters and a visible energy of at least $0.4 \cdot \sqrt{s}$. The presence of an isolated lepton is required. Electron candidates are identified as a track with an associated cluster in the electromagnetic calorimeter, muon candidates are identified as tracks in the muon spectrometer, while tau leptons are identified as low multiplicity jets comprising either 1 or 3 tracks. The energy of the lepton must be at least 10 GeV, while its polar angle should be at least $15°$ away from the beam direction. All clusters in the event, except the ones associated to the reconstructed lepton, are combined to form two hadronic jets using the DURHAM algorithm [29]. The energy of the most energetic jet, assumed to be the one originating from the $b-$ quark, is required to exceed 40 GeV. Finally, the missing momentum vector must be at least $26°$ away from the beam axis.

To further reject events from WW and qq background, the missing momentum is required to exceed 25 GeV and the invariant mass M_{qq} must be less than 65 GeV. In addition, the width of the broad jet, defined as the sum of the transverse momenta of the jet clusters scaled to the jet energy, must be less than 0.4. Finally, the relations (6) and (7) are used to obtain the top mass as a function of the measured energies of the jets, $M_t(E_c)$ and $M_t(E_b)$. In order to select the signal region, $M_t(E_c)$ and $M_t(E_b)$ are required to exceed 140 and 160 GeV, respectively. After applying all these cuts, 88 events are left in the data sample, with 90.8 expected from Standard Model background, while the efficiency on the signal is 11.6 % [3)]

In order to enhance the separation between signal and background, a neural network technique [30, 31] is used. The most important event variables are used as inputs to a feed-forward neural network; it consists of one layer with 12 input nodes, one layer of 25 hidden nodes and three output nodes, NN_{tc}, NN_{WW}, NN_{qq}, used for the signal, the WW and qq background, respectively. The final variable is then obtained as the product $NN = NN_{tc} * (1 - NN_{WW}) * (1 - NN_{qq})$. The input variables are related to the missing energy (module and direction of missing momentum vector), the btag of the most energetic jet, the invariant masses of the pairs jet-jet and lepton-neutrino, and to the top mass reconstructed from the jet energies, $M_t(E_c)$ and $M_t(E_b)$.

The distributions of the most relevant variables are shown in Figures 2 to 5, for an energy range from 192 GeV to 202 GeV; the signal expectations are for an arbitrary cross section $\sigma(e^+e^- \to t\bar{c} \to b\bar{c}l\nu) = 200fb$. A general good agreement is observed between the data and the Standard Model background expectations. The distribution of the final variable $NN = NN_{tc} * (1 - NN_{WW}) * (1 - NN_{qq})$ obtained from the neural network is shown in Figure 6, showing a good agreement between data and background, and a very good discriminating power between signal and background. No excess is found with respect to Standard Model expectations.

3.2 Hadronic Channel

The signature for this channel are four hadronic jets. One of them contains the c leading quark and its mean energy is expected at about 17 GeV (Equation 6). Another jet contains the b quark with an expected mean energy of about 70 GeV (Equation 7). Forcing the jet reconstruction algorithm to build four jets events, we define the c-jet as the one with the lowest energy, the b-jet being the one with the best btag. The non-c and non-b jets are used to reconstruct the W. For this channel, the main backgrounds are W^+W^- production and QCD events.

We first applied an hadronic preselection, where we required a visible energy of at least $0.7 \times \sqrt{s}$ and an effective center-of-mass energy of at least $0.85 \times \sqrt{s}$. We also require more than 20 reconstructed tracks and more than 2 jets built using the DURHAM algorithm [29] with a y_{cut} of 0.02. A background rejection is then applied, requiring an event thrust less than 0.82 (Figure 7), the reconstructed W mass must be 10 GeV around 80 GeV ($|M_W(rec) - 80| < 10$, Figure 8). To further reject W^+W^- background, a neural network with 4 inputs (Figure 9), 20 hidden nodes and 3 output is used, as in the leptonic case, the discriminating variable is the product $NN = NN_{tc} * (1 - NN_{WW}) * (1 - NN_{qq})$, which is required to be larger than 0.1 (Figure 10). Cuts are also applied on the c-jet mass (less than 5 GeV, Figure 11) and on the b-jet btag (large than 0.35, Figure 12). At this stage, the final sample statistics is: 79 data events, 76.2 background expected and 11.5 % of efficiency on signal [4)]. No excess is found with respect to Standard Model expectations.

[3)] Here the signal efficiency is multiplied by the leptonic W decay branching ratio.

[4)] Here the signal efficiency is multiplied by the hadronic W decay branching ratio.

For this channel we use a final variable similar to a likelihood from the signal to noise ratio:

$$\text{final variable} = \prod_{k=1}^{nvar} \frac{\epsilon^k_{signal}(x^k)}{N^k_{back}(x^k)} \tag{8}$$

Where ϵ^k_{signal} and N^k_{back} are the signal efficiency and the background expectation corresponding to a value x^k of variable k. The variables used are the b-jet energy and btag, the c-jet mass, the reconstructed top mass (Figure 13) and the two jet invariant mass. The final variable distribution is shown in Figure 14.

4 Results

The likelihood as a function of the number of expected signal events is determined from the distributions of the final variable for each analysis. Poisson statistics for the number of observed data events is used to define the estimator [32, 33]:

$$F(s,b,n) = e^{-(s+b)} \prod_{j=1}^{k} \frac{(s_j+b_j)^{d_j}}{d_j!} \tag{9}$$

The index j runs over the different bins of the distribution, s_j, b_j and d_j are the number of signal, background and data events which are in the channel j, while s and b are the total number of signal and background events. Using the Bayesian approach, the confidence level for a given number of expected signal event S is obtained with the following integration:

$$1 - CL = \frac{\int_S^\infty F(s,b,d)ds}{\int_0^\infty F(s,b,d)ds} \tag{10}$$

From this expression a 95% confidence level upper limit to the total single top production cross section is derived.

Using the distributions of the final discriminating variables, shown in Figures 6 and 14, the following 95 % CL upper limits in picobarn are found (those results are preliminary):

	Leptonic	Hadronic	Combined
σ measured	0.162 pb	0.344 pb	0.136 pb
σ expected	0.199 pb	0.324 pb	0.160 pb

5 Conclusions

A search for FCNC top-charm production has been performed, using the 410 pb^{-1} data sample collected by the L3 experiment at LEP 2, at a mean energy of 193.3 GeV. No evidence of excess with respect to the Standard Model expectations is found. Two independent channels have been analysed; combining the results of both channels, the following preliminary limit on single top production cross section has been obtained:

$$\sigma(e^+e^- \to t\bar{c}) < 136 \text{ fb} \quad \text{at } 95\ \%\ CL \tag{11}$$

Using the anomalous couplings formalism described in [9], and the cross section expression (5), one get an exclusion region in the $k_\gamma\ -\ k_Z$ plane, shown in Figure 15. Our results improve the CDF limits [8].

The results presented here improve and supersedes our previous results [34]

References

[1] G. Eilam and J. L. Hewett and A. Soni, Phys. Rev. **D44** (1991) 1473–1484.

[2] C-S Huang et al., Phys. Lett. **B 452** (1999) 143.

[3] Michael Luke and Martin J. Savage, Phys. Lett. **B307** (1993) 387–393.

[4] Chong Sheng Li and R. J. Oakes and Jin Min Yang, Phys. Rev. **D49** (1994) 293–298.

[5] Jorge L. Lopez and D. V. Nanopoulos and Raghavan Rangarajan, Phys. Rev. **D56** (1997) 3100–3106.

[6] V. Barger and M. S. Berger and R. J. N. Phillips, Phys. Rev. **D52** (1995) 1663–1683.

[7] Howard Georgi and Lev Kaplan and David Morin and Andreas Schenk, Phys. Rev. **D51** (1995) 3888–3894.

[8] F. Abe et al., Phys. Rev. Lett. **80** (1998) 2525–2530.

[9] V. F. Obraztsov and S. R. Slabospitsky and O. P. Yushchenko, Phys. Lett. **B426** (1998) 393–402.

[10] S. Bar-Shalom and J. Wudka, Phys. Rev. **D60** (1999) 094016.

[11] L3 Collaboration, B. Adeva et al., Nucl. Inst. Meth. **A 289** (1990) 35.

[12] J. A. Bakken et al., Nucl. Inst. Meth. **A 275** (1989) 81.

[13] O. Adriani et al., Nucl. Inst. Meth. **A 302** (1991) 53.

[14] B. Adeva et al., Nucl. Inst. Meth. **A 323** (1992) 109.

[15] K. Deiters et al., Nucl. Inst. Meth. **A 323** (1992) 162.

[16] M. Chemarin et al., Nucl. Inst. Meth. **A 349** (1994) 345.

[17] M. Acciarri et al., Nucl. Inst. Meth. **A 351** (1994) 300.

[18] G. Basti et al., Nucl. Inst. Meth. **A 374** (1996) 293.

[19] A. Adam et al., Nucl. Inst. Meth. **A 383** (1996) 342.

[20] L. Cuénoud, Générateurs de Flavour Changing Neutral Currents, Travail de diplôme, Université de Lausanne, 1996.

[21] T. Sjöstrand, "PYTHIA", Preprint TH/93-7112, CERN, 1993, Revised August 1995.

[22] T. Sjöstrand, Comp. Phys. Comm. **82** (1994) 74.

[23] M. Skrzypek et al., Comp. Phys. Comm. **94** (1996) 216.

[24] M. Skrzypek et al., Phys. Lett. **B 372** (1996) 289.

[25] S. Jadach and B. F. L. Ward and Z. Wąs, Comp. Phys. Comm. **66** (1991) 276.

[26] R. Brun et al., "GEANT 3", CERN DD/EE/84-1, Revised 1987.

[27] H. Fesefeldt, "GHEISHA", Preprint PITHA 85/02, RWTH Aachen, 1985.

[28] L3 Collaboration, M. Acciarri et al., Phys. Lett. **B 411** (1997) 373.

[29] S. Bethke et al., Nucl. Phys. **B 370** (1992) 310.

[30] L. Lönnblad and C. Peterson and T. Rognvaldsson, Nucl. Phys. **B 349** (1991) 675.

[31] C. Peterson et al., Comp. Phys. Comm. **81** (1994) 185.

[32] V. F. Obraztsov, Nucl. Inst. Meth. **A 316** (1992) 388.

[33] A. Favara and M. Pieri, "Confidence Level Estimation and Analysis Optimization", Preprint, INFN University of Florence, 1997, DFF-278-4-1997.

[34] The L3 Collaboration, "Search for Single Top Production at LEP 2", L3 Internal note 2506, 2000.

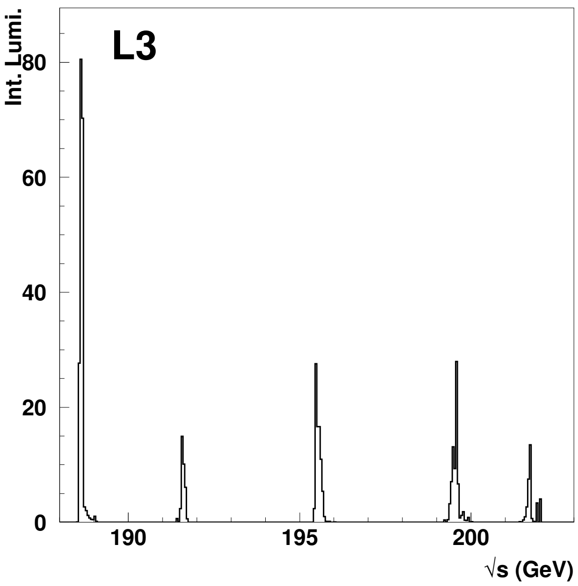

Figure 1: Distribution of the integrated luminosity collected by L3 during the years 1998 and 1999, in the center of mass energy range from 189 GeV to 202 GeV. 176.8 pb^{-1} have been collected at 189 GeV in 1998. 29.7 pb^{-1}, 83.7 pb^{-1}, 82.8 pb^{-1} and 37.0 pb^{-1} have been collected in 1999 at 192 GeV, 196 GeV, 200 GeV and 202 GeV respectively.

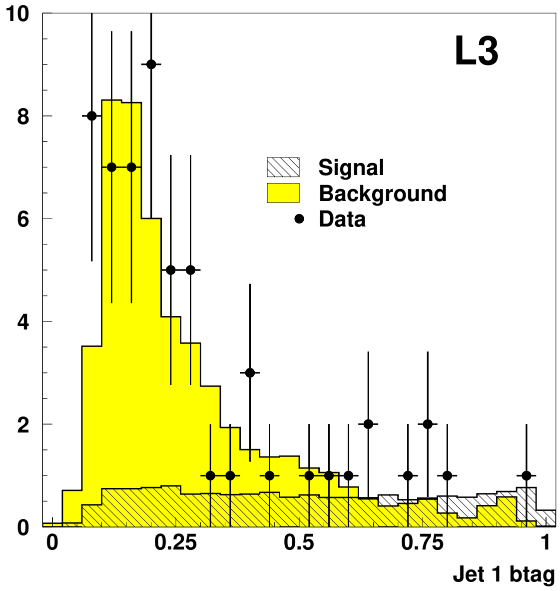

Figure 2: Leptonic channel: distribution of the btag variable for the most energetic jet.

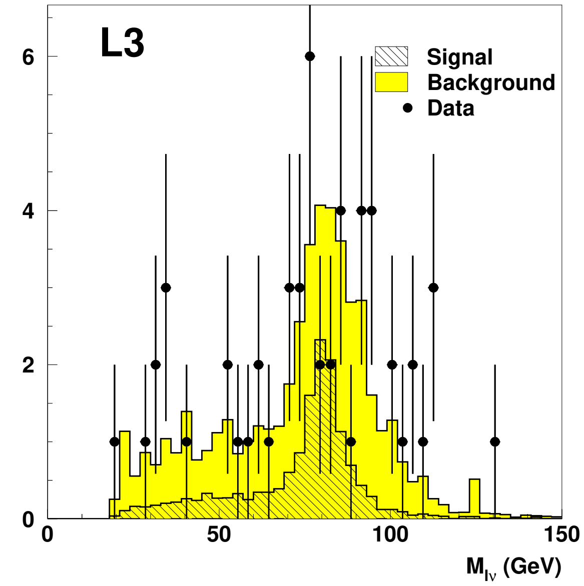

Figure 3: Leptonic channel: distribution of the invariant mass of the system lepton-missing momentum.

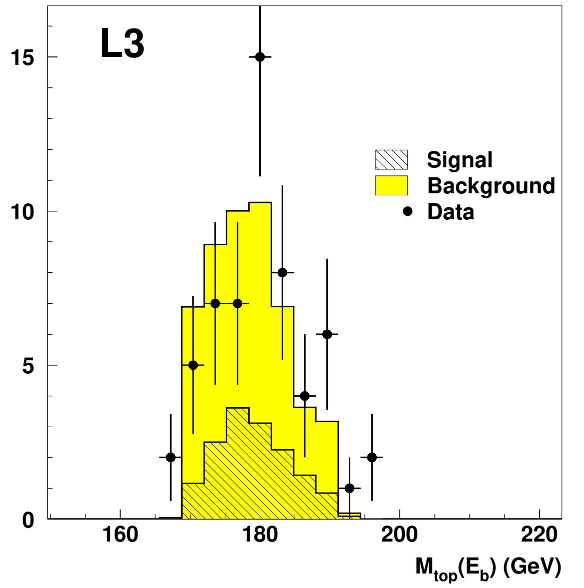

Figure 4: Leptonic channel: distribution of the top mass reconstructed from the b-jet energy (Equation 7).

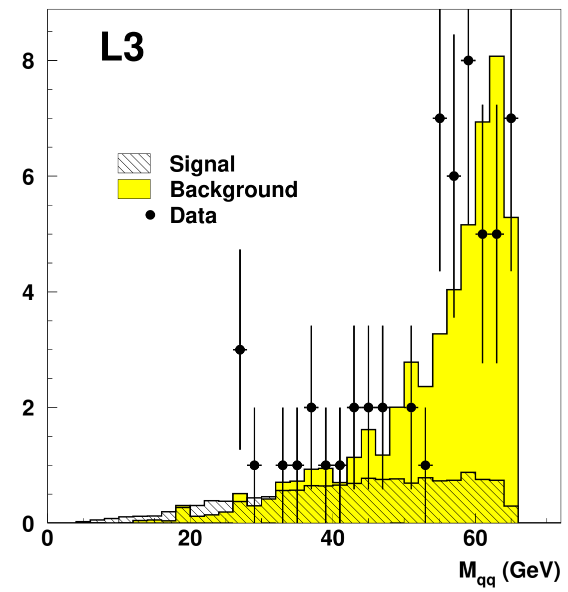

Figure 5: Leptonic channel: distribution of the invariant mass of the two jets.

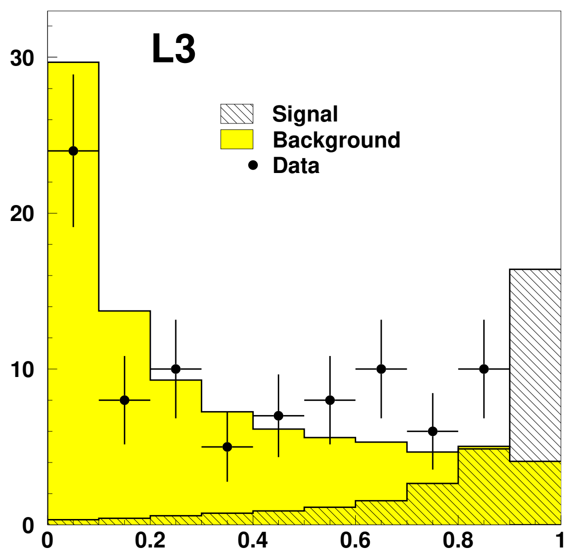

Figure 6: Leptonic channel: distribution of the final discriminating variable obtained from an artificial neural network.

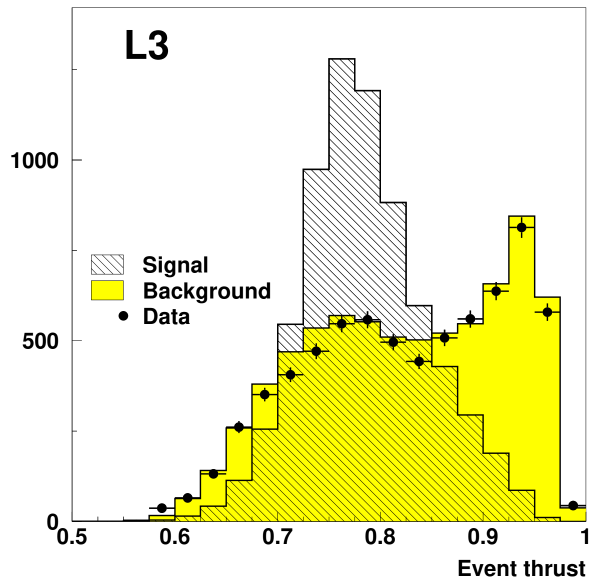

Figure 7: Hadronic channel: distribution of the event thrust, a cut at 0.82 is applied rejecting essentially QCD background.

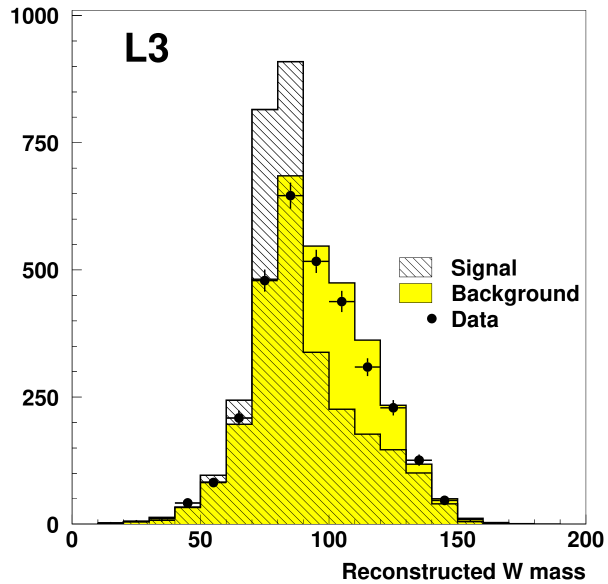

Figure 8: Hadronic channel: distribution of the reconstructed W mass

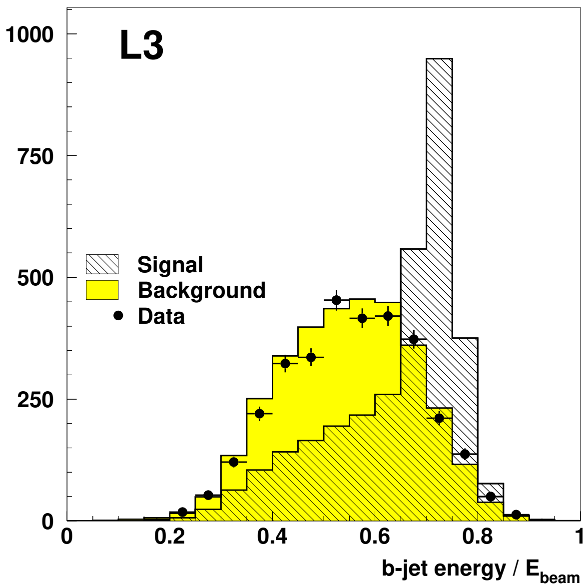

Figure 9: Hadronic channel: distribution of the b-jet energy normalized to the beam energy. This variable is used as input for the global neural network.

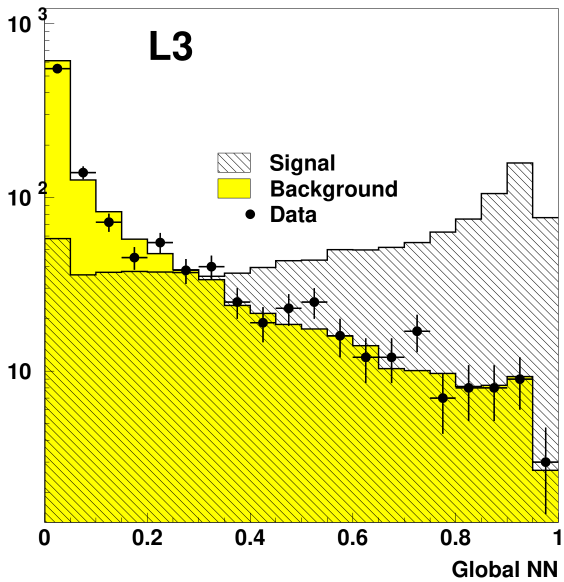

Figure 10: Hadronic channel: distribution of the neural network output, a cut at 0.1 is applied, rejecting W^+W^- background.

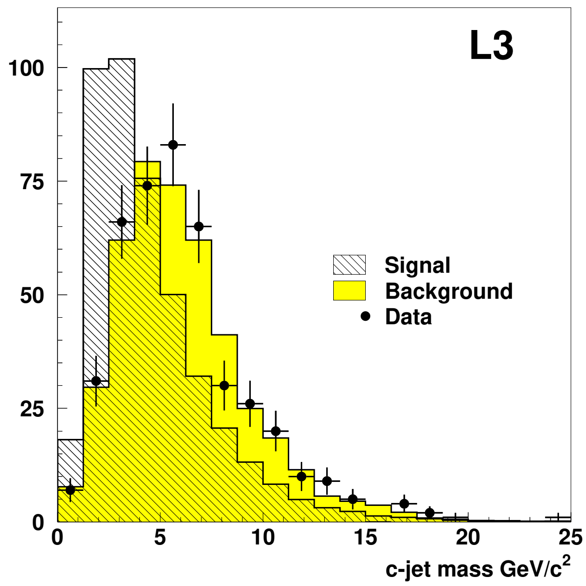

Figure 11: Hadronic channel: distribution of the c-jet mass.

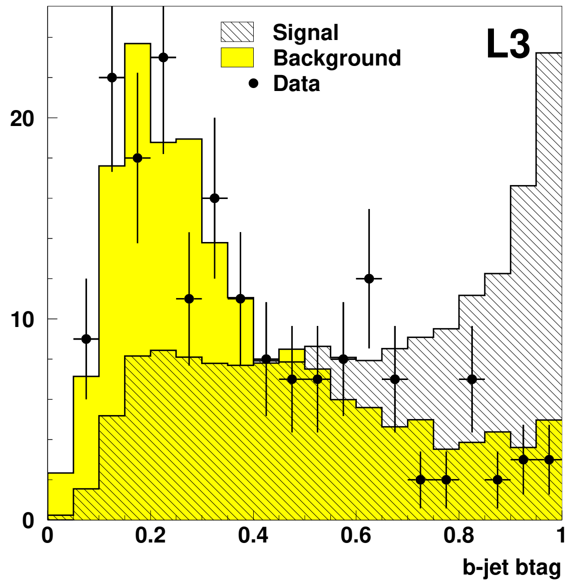

Figure 12: Hadronic channel: distribution of the b-jet btag variable. This variable is used as input for the global neural network.

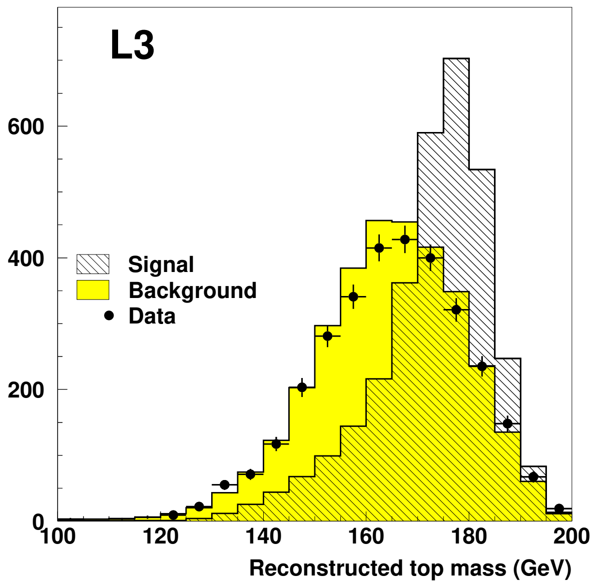

Figure 13: Hadronic channel: distribution of the reconstructed top mass

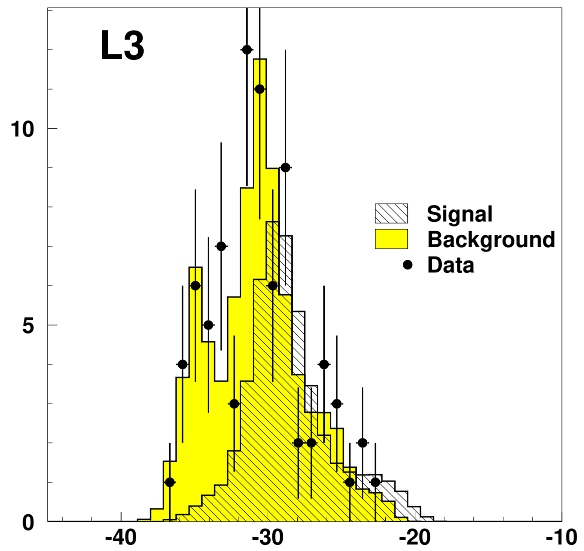

Figure 14: Hadronic channel: distribution of the final variable.

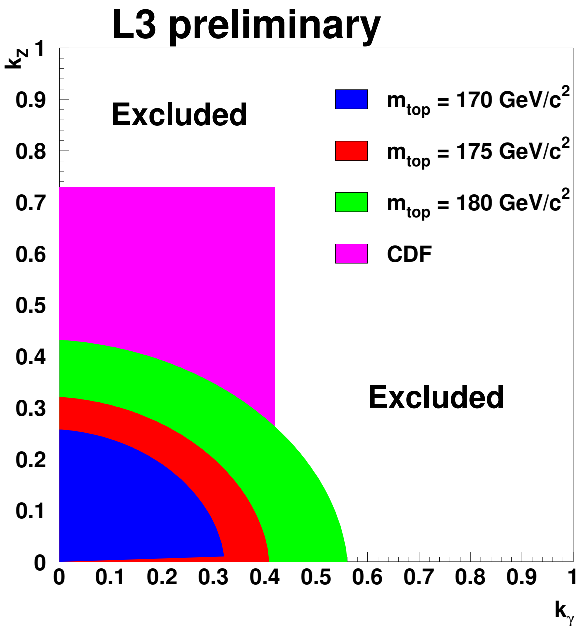

Figure 15: From the cross section expression 5, we get the exclusion curves at 95 % confidence level (CL) in the $k_\gamma - k_Z$ plane for three different values of the top mass m_{top}. The CDF exclusion domain is also shown.